Basics and prospective of magnetic Heusler compounds

Claudia Felser, Lukas Wollmann, Stanislav Chadov, Gerhard H. Fecher, and Stuart S. P. Parkin

---

Articles you may be interested in

Exchange-spring like magnetic behavior of the tetragonal Heusler compound Mn2FeGa as a candidate for spin-transfer torque
Appl. Phys. Lett. **102**, 202402 (2013); 10.1063/1.4807427

Structural and magnetic properties of the Heusler compound Fe2MnGa
J. Appl. Phys. **113**, 17E301 (2013); 10.1063/1.4794979

The zero-magnetization Heusler ferrimagnet
J. Appl. Phys. **113**, 17B101 (2013); 10.1063/1.4794744

Search for spin gapless semiconductors: The case of inverse Heusler compounds
Appl. Phys. Lett. **102**, 022402 (2013); 10.1063/1.4775599

Investigation of Co 2 Fe Si : The Heusler compound with highest Curie temperature and magnetic moment
Appl. Phys. Lett. **88**, 032503 (2006); 10.1063/1.2166205

Basics and prospective of magnetic Heusler compounds

Claudia Felser,[1,a] Lukas Wollmann,[1] Stanislav Chadov,[1] Gerhard H. Fecher,[1] and Stuart S. P. Parkin[2]

[1]*Max-Planck-Institut für Chemische Physik fester Stoffe, Nöthnitzer Str. 40, 01187 Dresden, Germany*
[2]*Max-Planck-Institut für Mikrostrukturphysik, Weinberg 2, Halle, Germany*

Heusler compounds are a remarkable class of materials with more than 1000 members and a wide range of extraordinary multi-functionalities including halfmetallic high-temperature ferri- and ferromagnets, multi-ferroics, shape memory alloys, and tunable topological insulators with a high potential for spintronics, energy technologies, and magneto-caloric applications. The tunability of this class of materials is exceptional and nearly every functionality can be designed. Co_2-Heusler compounds show high spin polarization in tunnel junction devices and spin-resolved photo-emission. Manganese-rich Heusler compounds attract much interest in the context of spin transfer torque, spin Hall effect, and rare earth free hard magnets. Most Mn_2-Heusler compounds crystallize in the inverse structure and are characterized by antiparallel coupling of magnetic moments on Mn atoms; the ferrimagnetic order and the lack of inversion symmetry lead to the emergence of new properties that are absent in ferromagnetic centrosymmetric Heusler structures, such as non-collinear magnetism, topological Hall effect, and skyrmions. Tetragonal Heusler compounds with large magneto crystalline anisotropy can be easily designed by positioning the Fermi energy at the van Hove singularity in one of the spin channels. Here, we give a comprehensive overview and a prospective on the magnetic properties of Heusler materials. © *2015 Author(s). All article content, except where otherwise noted, is licensed under a Creative Commons Attribution 3.0 Unported License.* [http://dx.doi.org/10.1063/1.4917387]

Materials for applications are becoming increasingly complex. The element-semiconductors silicon and germanium are widely used, but nowadays binary, ternary, and even quaternary semiconductors such as GaN,[1] $GaP_{1-x}As_x$,[2] or $Cu(GaIn)Se_2$[3] play an important role in electronics and materials for energy conversion. More elements allow for more degrees of freedom such as band-gap tuning and multi-functionality. Advances in understanding the chemistry, physics, and materials science have enabled the rational design of new functionalities for a plethora of advanced technologies. However, controlling disorder and defects and the availability of the elements in the earth's crust are increasingly a challenge for applications. In this article, we summarize current knowledge about magnetic half Heusler and Heusler compounds with a focus on potential applications in spintronics, for data storage, magnetocalorics, and permanent magnets. A more detailed description of the basic understanding of Heusler compounds is given in Ref. 4. The goal of the article is to discuss future prospective of the unique family of magnetic compounds.

Half Heusler compounds of the composition 1:1:1 with three inter-penetrating fcc-lattices and Heusler compounds of the composition 2:1:1 with four inter-penetrating fcc-lattices were discovered in 1903 by Heusler.[5,6] There is no clear definition of a Heusler compound:[4] the first Heusler compounds, namely, CuMnSb, Cu_2MnAl, and Cu_2MnSn, drew attention because they display ferromagnetic properties while being formed from non-magnetic elements.[5,6] These first Heusler

---

[a]Author to whom correspondence should be addressed. Electronic mail: felser@cpfs.mpg.de Tel.: +49-351-46 46 3004.

3, 041518-1

compounds all contain manganese, which plays a unique role in this class of materials. The appearance of unexpected properties that are not simply evolved from those of the elements from which the compounds are made off is an important distinction from common magnetic alloys. The fact that Heusler compounds are related to semiconductors and the unique role of manganese enables us to formulate rules for rational design.

Semiconducting half Heusler compounds can be understood as "stuffed" variants of the binary zinc blende semiconductor and by simple electron counting (Figures 1(a) and 1(b)). A good starting point is the Nowotny-Juza phases, which are relatives of the Heusler compounds.[4] This closely related set of compounds with the formula LiYZ has 3 interpenetrating fcc lattices and the sum of the valence electrons is eight, just like the binary semiconductors. The Z atom is always a nonmagnetic semiconducting or metallic element just as in the Heusler compounds. GaAs is a III V semiconductor and LiMgAs is a I II V semiconductor. The band gap in both compounds is similar, the gap is between the bonding and the antibonding *s*- and *p*-states and depends on the bonding strength between the atoms building the zinc-blende lattice. These common features are visualized in Figure 1. In the half Heusler compounds XYZ, the X atom is always the most electropositive atom from X, Y, and Z and together with the Z atoms forms a rock-salt (NaCl) like sub-lattice which reflects the more ionic bonds between X and Z. By contrast, the Y atoms and the Z atoms form a zinc blende like lattice which reflects a more covalent bonding situation. Examples of nonmagnetic semiconductors are ZrNiSn and LaPtBi, for which the total number of valence electrons is 18. Stable transition metal complexes such as $Ni(CO)_4$ also follow an 18 valence electron rule, with closed shell complexes formed from the 10 *d*-, 6 *p*-, and 2 *s*-electrons. A scheme of the density of states (DOS), including the occupied *d*-states, is shown in Figure 1(c). Although zirconium, nickel, and tin are metals, the resulting compound is a semiconductor and, moreover, a good thermoelectric material.[4] The band gap is a result of strong covalent bonding. One recent prominent example of a binary semiconductor—half Heusler compound analogue are the topological insulators. By analogy with the HgTe/CdTe quantum well structure,[7] topological insulators and a spin quantum Hall effect have been foreseen for half Heusler compounds.[8,9] The fingerprint of a topological insulator is a band inversion of the valence and conduction bands. Many of these compounds are non-centro-symmetric superconductors and, therefore, candidates for Majorana quasi-particles.[10] The challenges in the area of topological insulators are to grow quantum well structure of half Heusler compounds, take advantage of the multifunctionality to investigate quantum spin Hall effect and quantum anomalous Hall effect, and search for Majorana fermions and Kondo topological insulators.

The magnetic half Heusler compounds contain rare earth elements or manganese. Examples are GdNiSn, MnNiSb (or more commonly written as NiMnSb), YbPtBi, or PtMnBi, Figure 2(a). Rare earth atoms have a formal valence of RE^{3+} and contribute 3 valence electrons to the 18 valence
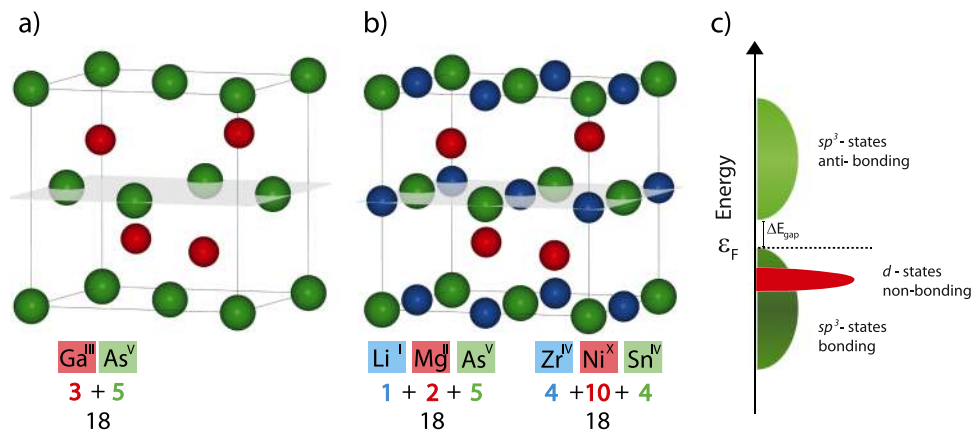

FIG. 1. (a) Zinc blende crystal structure, red spheres As, green spheres Ga; (b) half Heusler structure, red spheres Y=Ni, green spheres Sn, blue spheres Zr; (c) schematic DOS of ZrNiSn, green sp^3-bonding, and antibonding states, red d^{10}-states.
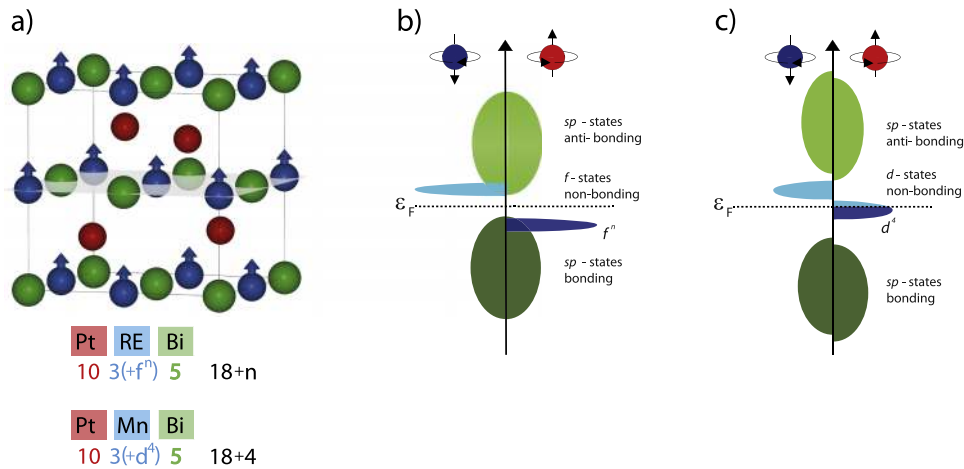
FIG. 2. (a) Magnetic half Heusler compounds, crystal structure, red spheres Pt, green spheres Bi, blue spheres Mn or Rare earth metals; (b) schematic DOS of LaPtBi; (c) schematic DOS of PtMnBi, blue f and d-states.

electrons. Manganese also behaves like a rare earth, Mn^{3+} in NiMnSb has a d^4 configuration, and results in a localized moment of 4 bohrs magnetons.[4] The magnetic moment of Ni is nearly zero. The magnetism in the half Heuslers arises from Mn or rare earth elements on the Y sites and is of the localized type (see Figures 2(b) and 2(c)). The Y sites are octahedrally coordinated with respect to the Z lattice. Rare earth containing half Heusler compounds are magnetic semiconductors or semimetals, and the corresponding Manganese compounds are so called half metallic ferromagnets.[4] The electronic structure and the electron counting rules are schematically shown in Figure 2. In 1983, de Groot recognized that NiMnSb has a unique band structure, insulating in the minority band but metallic in the majority spin band[11] and Kübler points out a similar band structure in the Co_2MnZ Heusler compounds.[12]

The Heusler compounds are ternary compounds with the chemical formula X_2YZ and a structure of the $L2_1$ or Cu_2MnAl (defined in the Pearson table) type.[13] The X and Y atoms are transition metals or lanthanides (rare-earth metals) and the Z sub-lattice is always formed by a main group metal or a semimetal. Sometimes, Heusler compounds are called full Heusler compounds, because in the fcc-lattice of the Z atoms, all voids (octahedral and tetrahedral) are filled. In half Heusler compounds, only half of the tetrahedral sites are filled. Semiconducting Heusler compounds are rare but exist with 8 (Li_2NaSb) or 18 valence electrons (Li_2CdGe) per formula unit valence electron concentration (VEC) analogous to the half Heusler compounds. The VEC is the sum of the electrons in the s-, p-, and d-electrons in the outer shell of the X, Y, and Z elements, just as for the half Heusler compounds. Even 24 VEC semiconductors are possible in case of three transition metals per formula unit.[4] As an example, Fe_2VAl is a non-magnetic semiconductor with non-magnetic iron (see Figure 3(a)).[14] Co_2YZ Heusler compounds have more than 24 VEC and follow the so called Slater-Pauling rule.[17–19] If the number of valence electrons differs from 24, then these materials are magnetic, where the magnetic moment per formula unit is directly related to the number of valence electrons minus 24. An important distinction from the half Heusler compounds is that the full Heusler compounds have two distinct magnetic sub-lattices. Kübler was the first to appreciate that the magnetism on the Y sites is of the localized type, whereas the magnetism of the Cobalt is delocalized. As an example, the magnetic structure and the density of states of Co_2FeSi are illustrated in Figure 3(b): the exchange interaction between the cobalt and iron atoms is ferromagnetic.[17–19] For the ferromagnetic halfmetallic Heusler compounds, the Curie temperature is proportional to the number of valence electrons per formula unit above 24 and the Curie temperature increases by ~175 K per added electron.[20,21] For example, Co_2TiSn (26 valence electrons with a saturation magnetization of 2 μ_B/formula unit) is ferromagnetic with a magnetic moment that mainly resides on the Co sites with a Curie temperature of ~350 K.[22] All Co sites are identical in this compound. Another example is Co_2FeSi. This compound is also ferromagnetic but with magnetic moments

a) Fe$_2$VAl   b) Co$_2$FeSi   c) Mn$_2$VAl
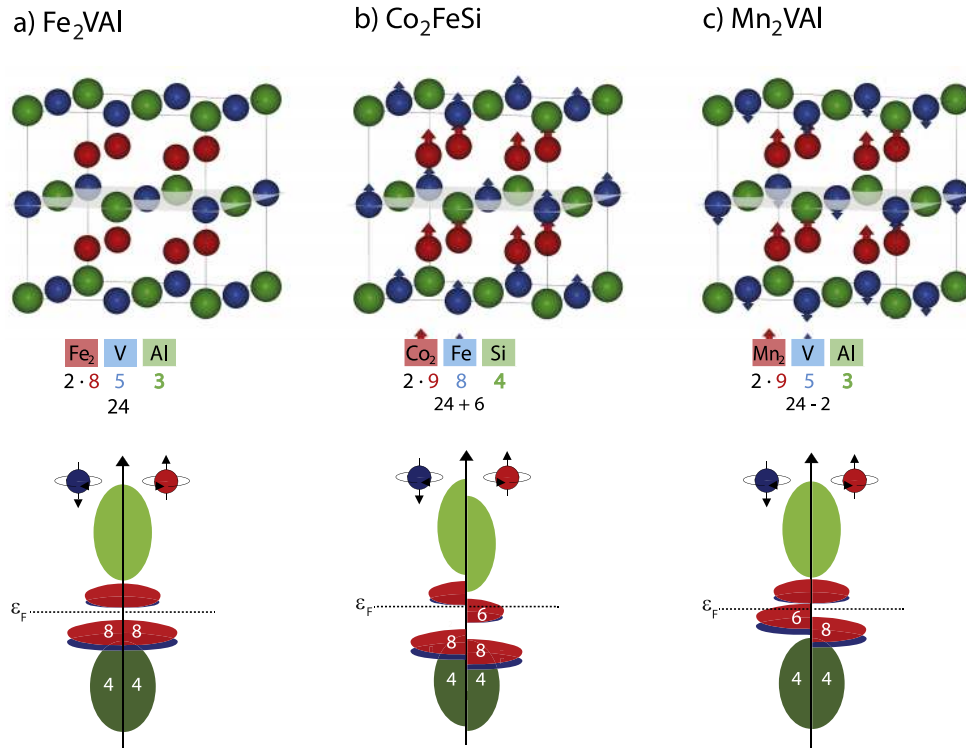

FIG. 3. (a) Nonmagnetic Heusler compounds, crystal structure, red spheres Fe, green spheres Al, blue spheres V (upper panel) of Fe$_2$VAl and schematic DOS (lower panel); (b) ferromagnetic Heusler compounds Co$_2$FeSi, crystal structure, red spheres Co, green spheres Si, blue spheres Fe with spin orientation on the magnetic atoms (upper panel) and schematic DOS (lower panel); (c) ferrimagnetic Heusler compounds Mn$_2$VAl, crystal structure, red spheres Mn, green spheres Al, blue spheres V with spin orientation on the magnetic atoms (upper panel) schematic DOS (lower panel).

on both the Co and Fe atoms. This compound has the highest Curie temperature of any known Heusler compound, ~1120 K.[19] Slater-Pauling behavior is a sign of bulk halfmetallicity (100% spin polarization) in that varying the number of valence electrons varies the filling of the metallic spin polarized band so that the moment is increased or decreased in direct proportial to the number of valence electrons.[15–17,23] This is true as long as the Fermi energy remains within the energy gap of the semiconducting spin-polarized band. The compounds that follow the Slater-Pauling rule typically contain Co, Mn, or Fe atoms on the X and/or Y sites.

Co$_2$(CrFe)Al (CCFA) was the first compound for which a high magnetoresistance as a signature for a high spin polarization was found at room temperature.[24,25] The highest tunnel magnetoresistance of more than 2000% was observed in the Heusler compounds Co$_2$MnSi with excess of manganese.[26] For the same compound, a high spin polarization was proven directly by spin-polarized photoemission.[27] In the following, it will become clear why Co and Mn are an excellent combination to achieve a high spin polarization. Many of the cubic Co$_2$YZ are half metallic ferromagnets, whereas Fe$_2$YZ compounds often exhibit a deviation from the Slater Pauling rule due to disorder or less localized states at the Fermi energy. The Co$_2$-Heusler compounds are well understood and the interface with MgO and local order is "under control." To use the materials now in real devices and to inject spins into semiconductors including all Heusler devices are the future challenges.[28]

One of the few examples of a half metallic Mn$_2$-Heusler compound with *ferro*magnetic coupling between the two manganese atoms is Mn$_2$VAl,[29] with less than 24 VEC (see Figure 3(c)). Most of the Mn$_2$YZ compounds are very different from Co$_2$YZ and Mn$_2$VAl and crystallize in the inverse Heusler structure,[4] where the manganese moments sitting on two different sites are coupled parallel to one another[30,31] (each Mn sits on a crystallographically distinguishable site, as
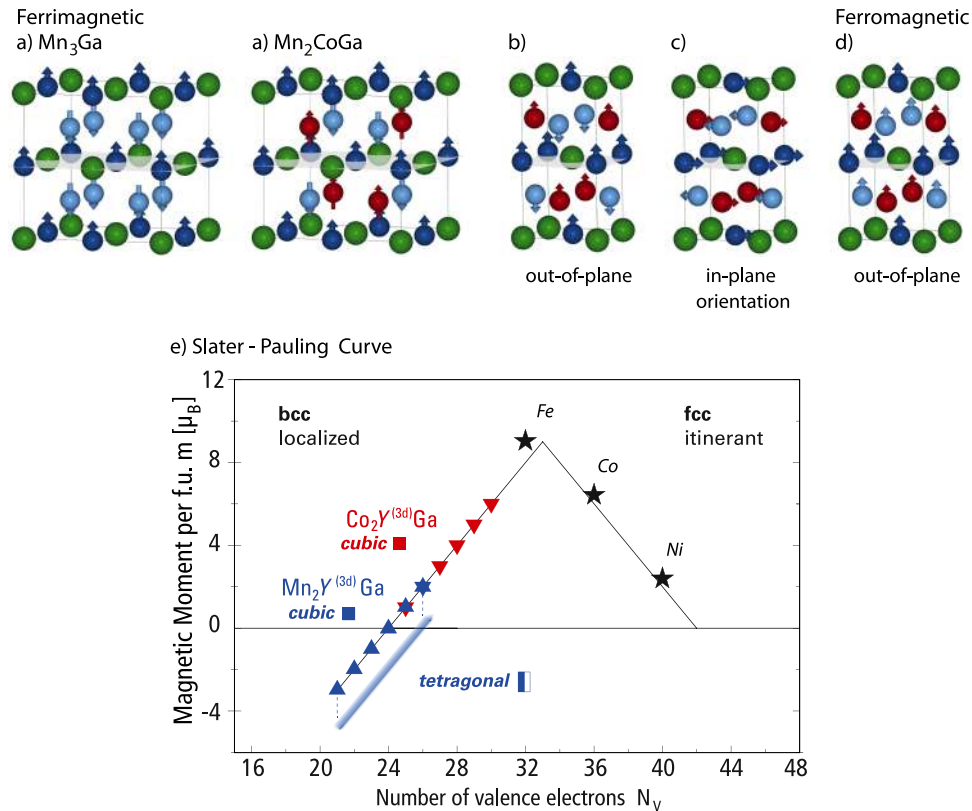
FIG. 4. (a) Crystal structure of cubic compensated ferromagnetic Mn_3Ga, blue and light blue spheres Mn, green spheres Ga with spin orientation on the magnetic atoms, and cubic ferromagnetic Mn_2CoGa with the inverse Heusler structure blue spheres Mn and red spheres Co, green spheres Ga with spin orientation on the magnetic atoms. (b) Ferrimagnetic tetragonal inverse Heusler compounds such as Mn_2RhSn, red spheres Rh, green spheres Sn, blue and light spheres Mn with out-of-plane spin orientation on the magnetic atoms and (c) with in-plane spin orientation and (d) ferromagnetic out-of-plane spin orientation; (e) Slater-Pauling curve for cubic Co2YZ (red triangles), cubic Mn_2YZ (blue triangles), and tetragonal Mn_2YZ (blue line).

illustrated in Figure 4). Cubic Mn_3Ga with 24 valence electrons is a "borderline compound" and is a fully compensated ferrimagnet[30–32] principally different from non-magnetic semiconductors like Fe_2VAl due to the special role of manganese in Heusler compounds.[12,30] The magnetic moments on the different sites have different magnetization directions, which lead to a complete compensation of the magnetic moments, see Figure 4(a). Another example of a *ferri*-magnetic inverse Heusler compound is Mn_2CoAl or better (MnCo)MnAl in which the Mn moment on the octahedrally coordinated Y site has a localized moment with an approximate "d^4-configuration" and the manganese and cobalt (MnCo) on the tetrahedrally coordinated site has a lower moment of ~2 μ_B. The two manganese atoms on different sites are coupled antiparallel, and the Co on the tetrahedral site is coupled to the Mn on the octahedral side parallel, similar like in Co_2MnZ compounds. However, the total moment still follows the Slater-Pauling rule with 26 valence electrons; the ferrimagnetic compound shows a net magnetic moment of 2 μ_B. The explanation is that the octahedral site is always occupied by the most electropositive element (i.e., the earlier transition metal, so, for example, here Mn rather than Co), so that this arrangement leads to an occupancy of half of the Mn and the Co on the tetrahedral site. These special compounds in which Mn occupies both the octahedral sites (Y) and is ordered on half of the tetrahedral sites (X) have lower space group symmetry (216 rather than 225) and are called inverse Heuslers (Figure 4(a)). They have no inversion symmetry as compared to the Co_2-Heuslers compounds.[4] Mn_2CoAl is an exceptional compound and is a spin gapless semiconductor with a Curie temperature of 720 K and an anomalous Hall effect, which is comparatively low, and which is explained by the symmetry properties of the Berry curvature.[33]

Most of the cubic ferrimagnetic Mn_2YZ still follow the Slater Pauling rule.[32,34] For the ferromagnetic halfmetallic Heusler compounds, the Curie temperature is related to the number of valence electrons.[20,21] For the ferrimagnetic halfmetallic Heusler compounds, the Curie temperature scales approximately with the sum of the magnetic moments of the two anti-parallel sub-lattices. All cubic Heusler compounds are naturally soft magnetic due to the vanishingly small magnetocrystalline anisotropy energy (MAE). At the same time, the magnetization values of the *ferro*magnetic Co_2- and Fe_2-Heusler compounds are high, whereas of the *ferri*magnetic Mn_2-Heusler compounds are low.[34]

For many applications such as spin transfer torque magnetic random access memory (STT-MRAM),[35,36] ultrahigh density magnetic recording applications,[37] and rare earth free permanent magnets, a high MAE is needed.[38] Anisotropic crystal structures such as tetragonally distorted Heusler compounds are a precondition for uniaxial magneto-crystalline anisotropy. The martensitic to austenitic phase transition in shape memory alloys and magneto-caloric Heusler compounds is phase transitions from an anisotropic (tetragonal, orthorhombic, or complex modulated structures) to an isotropic cubic structure.[39]

Mn_3Ga and $Mn_{3-x}Ga$ possess the stable tetragonal structure at ambient conditions,[31,40,41] as well as the perpendicular magnetization of their thin film electrodes, which suggests them as potential candidate materials for the STT RAM devices.[42–44] In general, Heusler compounds with low saturation magnetic moment, high magnetic crystalline anisotropy, low Gilbert damping, but high spin-polarization and high Curie temperature, are required to minimize the switching current and increase the switching speed in STT-MRAM devices according to the Slonczewski-Berger equation.[35,36] Unfortunately, a suitable interface between the tunneling barrier and the electrode is still a challenge[45] and only low tunneling magneto-resistance effects have been observed so far.[46,47] However, the material $Mn_{3-x}Ga$ shows a high MAE and THz oscillation, which makes it a potential candidate for spin torque oscillators.[48]

Besides the Curie temperature, the quality of the hard magnets is characterized by the maximum energy product $B \times H_{max}$. To maximize it, both strong coercive field and high magnetization are necessary. Large MAE in tetragonal Heusler compounds gives the first important ingredient to realize such high coercive fields. The high coercive field is naturally provided by the fully compensated tetragonally distorted ferrimagnets, as it is inversely proportional to the magnetization, which is vanishingly small, and directly proportional to the MAE, which is relatively large due to the tetragonal distortion.[49]

From the Slater Pauling curve in Figure 4 and from Wurmehl *et al.*,[30] it is obvious that the rational design of compensated ferrimagnets in cubic and tetragonal is possible, and first examples are already synthesized.[30,50,51]

There are at least three reasons why full Heusler compounds undergo a tetragonal distortion. One reason is that there is a Jahn-Teller ion on the Y site, such as, for example, Mn^{3+}. The Mn^{3+} has a d^4 configuration, which is a typical configuration for a Jahn-Teller distortion.[52,53] A Jahn-Teller configuration is an electronic configuration with degenerate orbitals, which are partially filled so a structural distortion can lift the electronic degeneracy and lower the total energy of the system. The tetragonal distortion on the Y site affects the Z site by distorting the local tetrahedral environment. If there is Si on the Z site, there is no tetragonal distortion of the unit cell because Si prefers a highly symmetric tetrahedral environment and a sp^3 hybridization. Typically, Heusler compounds with Al, Ga, Ge, Sn, Pb, and Sb on the Z site allow for a tetragonal distortion in connection with Mn on the Y site. The octahedron can expand or shrink along one axis. Examples of Jahn-Teller driven tetragonally distorted Heuslers are manganese-rich Heusler compounds.[53] So far, all ferromagnetic manganese-rich Heusler compounds and their relatives show a perpendicular magnetization in thin films, as predicted by theory (Figure 4). The second reason why a Heusler or half Heusler can exhibit a tetragonal distortion is a van Hove singularity in the electronic band structure of the cubic magnetic compound: this is also called sometimes a band Jahn-Teller effect. The van Hove singularity is a saddle point in the electronic band structure at the Fermi energy which leads to a high density of states. Thus, a structural distortion which opens a gap, or more often a pseudo-gap, in the band structure can lower the energy of the system. By pseudo-gap we mean that not all the bands may exhibit an energy gap after the distortion. Examples of known tetragonally distorted Heuslers

compound are the magnetic shape memory compounds: Ni_2MnGa and Mn_2NiGa[55,56] and Rh_2FeSn, Rh_2CoSn, and Rh_2FeSb.[57] However, films of the Rh_2-compounds show in-plane magnetization,[58] in accordance with theory.[54] At high temperature and in a high magnetic field, these materials are cubic (austenite phase).[59] Jahn Teller and van Hove can play a role in the same system since a degenerate state goes along with a high density of states as, for example, in Mn_3Ga. The third reason why there could be a tetragonal distortion is spin-orbit coupling. This is the case for 4d or 5d transition metals on the tetrahedral (X) sites because high Z atoms are needed for strong spin-orbit coupling. Known compounds are, for example, Mn_2PtSn and Mn_2RhSn,[60,61] for structure see Figure 4(b). An example of a van Hove singularity-driven, tetragonally distorted Heusler with spin-orbit coupling is Rh_2FeSn.[57] The known tetragonally distorted Heusler compounds crystallize, for example, in the following structural classes: 119 (I-4m2), 139 (I4/mmm), e.g., Ni_2MnGa and Rh_2CoSn, 129 (P4/mmm), and 131 (P42/mmc).[1]

The magnetic structure of the Mn_2-Heusler compounds is distinguished from the Co_2-Heusler compounds, although both families follow the Slater Pauling curve, independent of the structure type, and continuous across the compensation point[34] (see Figure 4(e)). The magnetism in Mn_2-Heuslers is different for compounds with less or more than 24 VEC. As mentioned above, Mn_2VAl with 22 VEC is an itinerant ferromagnet; the manganese on the tetrahedral sites couples parallel to one another. Mn_3Ga with 24 VEC is a compensated ferrimagnet. As discussed in detail by Wollmann *et al.*,[34] the total magnetization is made up of contributions of different characters (localized or itinerant) for the Heusler and the inverse Heusler structure types. Regarding the large constant localized moment, Mn is thus the only 3d transition metal element in inverse Heusler compounds that behaves like a rare-earth element. Wollmann *et al.* believe the antiferromagnetic coupling of the two types of Mn atoms in the inverse Heusler compounds is due to direct exchange being an atomic property of Mn as in the elementary metal; the half-filled d shell leads to antiparallel coupling. Due to the antiparallel coupling for most of the manganese-rich Heusler compounds, the total magnetic moment is low, independent of the structure. In the tetragonally distorted Mn_2-Heusler compounds, the magnetic interaction does not change qualitatively, only the total magnetization is reduced, based on the over-compensation of the moments on the tetrahedral site versus the moments on the octahedral site. Therefore, the compounds do no fall on the Slater Pauling curve. The curve of the total moments is shifted by approximately 1 μ_B, as can be seen in Figure 4(e).

The challenge for STT-MRAM and permanent magnets is to find tetragonal Heusler compounds with high magnetic moments, i.e., ferromagnetic coupling between the magnetic sublattices, see Figure 4(d). Based on our knowledge today, it should be possible to design new tetragonal compounds with larger magnetic moments, but it might be difficult at first sight to design ferromagnetic Heusler compounds. In Mn_2-Heusler compounds, ferromagnetism might be metastable: a hint is the large exchange bias that has recently been observed in the new tetragonal Heusler compound $Mn_{2-x}Pt_{1-x}Ga$, after zero-field cooling from the paramagnetic state. First-principles calculations and magnetic measurements reveal that Mn_2PtGa orders ferrimagnetically with some ferromagnetic inclusions.[51] The non-centrosymmetric Mn_2RhSn is a novel non-collinear tetragonal Heusler compound that exhibits an unusually strong canting of its magnetic sub-lattices.[61] It undergoes a spin-reorientation transition, induced by a Dzyaloshinskii-Moriya exchange interaction. Mn_2RhSn and related compounds are promising candidates for realizing the skyrmion state in the Heusler family.[61]

Of the large number of potential tetragonally distorted Heusler compounds, including quaternary alloys, only a few are known, and the search for new compounds and a deeper understanding of the relationship between their electronic structure, magnetism, and crystal structure will likely have a high impact for all of the technological applications discussed in this article.

[1] J. Goldberger, R. He, Y. Zhang, S. Lee, H. Yan, H. J. Choi, and P. Yang, Nature **422**, 599-602 (2003).
[2] M. Teicher, R. Beserman, M. V. Klein, and H. Morkoç, Phys. Rev. B **29**, 4652 (1984).
[3] S. R. Kodigala, Cu(In$_{1-x}$Ga$_x$)Se$_2$ *Based Thin Film Solar Cells, Thin Films and Nanostructures*, 1st ed. (Academic Press, 2010).

[4] T. Graf, C. Felser, and S. S. P. Parkin, Prog. Solid State Chem. **39**, 1 (2011).

[5] F. Heusler, W. Starck, and E. Haupt, Verh. DPG **5**, 220 (1903).

[6] F. Heusler, Verh. DPG **5**, 219 (1903).

[7] M. König, S. Wiedmann, C. Brüne, A. Roth, H. Buhmann, L. Molenkamp, X.-L. Qi, and S.-C. Zhang, Science **318**, 766 (2007).

[8] S. Chadov, X. L. Qi, J. Kübler, G. H. Fecher, C. Felser, and S. C. Zhang, Nat. Mater. **9**, 541 (2010).

[9] H. Lin, L. A. Wray, Y. Xia, S. Xu, S. Jia, R. J. Cava, A. Bansil, and M. Z. Hasan, Nat. Mater. **9**, 546 (2010).

[10] L. Fu and C. L. Kane, Phys. Rev. Lett. **100**, 096407 (2008).

[11] R. A. de Groot, F. M. Mueller, P. G. v. Engen, and K. H. J. Buschow, Phys. Rev. Lett. **50**, 2024 (1983).

[12] J. Kübler, A. R. William, and C. B. Sommers, Phys. Rev. B **28**, 1745 (1983).

[13] *Pearson's Handbook of Crystallographic Data for Intermetallic Phases,* edited by Pierre Villars and Karin Cenzual, 2nd ed. (ASM International, Materials Park, Ohio, 2009).

[14] Y. Nishino, M. Kato, S. Asano, K. Soda, M. Hayasaki, and U. Mizutani, Phys. Rev. Lett. **79**, 1909 (1997).

[15] I. Galanakis, P. H. Dederichs, and N. Papanikolaou, Phys. Rev. B **66**, 174429 (2002).

[16] I. Galanakis, P. Mavropoulos, and P. H. Dederichs, J. Phys. D: Appl. Phys. **39**, 765 (2006).

[17] H. C. Kandpal *et al.*, J. Phys. D: Appl. Phys. **40**, 1507 (2007).

[18] S. Wurmehl *et al.*, Phys. Rev. B **72**, 184434 (2005).

[19] C. G. F. Blum *et al.*, Appl. Phys. Lett. **95**, 161903 (2009).

[20] J. Kübler, J. Phys. Condens. Matter **18**, 9795 (2006).

[21] J. Kübler, G. H. Fecher, and C. Felser, Phys. Rev. B **76**, 024414 (2007).

[22] H. C. Kandpal, V. Ksenofontov, M. Wojcik, R. Seshadri, and C. Felser, J. Phys. D: Appl. Phys. **40**, 1587 (2007).

[23] C. Felser, G. H. Fecher, and B. Balke, Angew. Chem., Int. Ed. **46**, 668 (2007).

[24] T. Block, C. Felser *et al.*, J. Solid State Chem. **176**, 646 (2003).

[25] K. Inomata, S. Okamura, R. Goto, and N. Yezuka, Jpn. J. Appl. Phys., Part 2 **32**, L419 (2003).

[26] H. X. Liu *et al.*, Appl. Phys. Lett. **101**, 132418 (2012).

[27] M. Jourdan *et al.*, Nat. Commun. **5**, 3974 (2014).

[28] S. Chadov *et al.*, Phys. Rev. Lett. **107**, 047202 (2011).

[29] C. Jiang, M. Venkatesan, and J. M. D. Coey, Solid State Commun. **118**, 513 (2001).

[30] S. Wurmehl, H. C. Kandpal, G. H. Fecher, and C. Felser, J. Phys.: Condens. Matter **18**, 6171 (2006).

[31] B. Balke, G. H. Fecher, J. Winterlik, and C. Felser, Appl. Phys. Lett. **90**, 152504 (2007).

[32] I. Galanakis, K. Özdoğan, E. Şaşıoğlu, and B. Aktaş, Phys. Status Solidi A **205**, 1036 (2008).

[33] S. Ouardi, G. H. Fecher, J. Kübler, and C. Felser, Phys. Rev. Lett. **110**, 100401 (2013).

[34] L. Wollmann *et al.*, Phys. Rev. B **90**, 214420 (2014).

[35] J. C. Slonczewski, J. Magn. Magn. Mater. **159**, L1 (1996).

[36] L. Berger, Phys. Rev. B. **54**, 9353 (1996).

[37] D. Weller *et al.*, IEEE Trans. Magn. **36**, 10 (2000).

[38] J. M. D. Coey, J. Phys.: Condens. Matter **26**, 064211 (2014).

[39] P. J. Webster, K. R. A. Ziebeck, S. L. Town, and M. S. Peak, Philos. Mag. Part B **49**, 295 (1984).

[40] J. Winterlik *et al.*, Phys. Rev. B **77**, 054406 (2008).

[41] E. Kren and G. Kadar, Solid State Commun. **8**, 1653 (1970).

[42] F. Wu, S. Mizukami, D. Watanabe, H. Naganuma, M. Oogane, Y. Ando *et al.*, Appl. Phys. Lett. **94**, 122503 (2009).

[43] M. Glas *et al.*, J. Magn. Magn. Mater. **333**, 134 (2013).

[44] A. Köhler *et al.*, Appl. Phys. Lett. **103**, 162406 (2013).

[45] C. E. V. Barbosa, S. Ouardi, T. Kubota, S. Mizukami, G. H. Fecher, T. Miyazaki, X. Kzina, E. Ikenaga, and C. Felser, J. Appl. Phys. **116**, 034508 (2014).

[46] T. Kubota *et al.*, Appl. Phys. Express **4**, 043002 (2011).

[47] T. Kubota *et al.*, Appl. Phys. Express **5**, 043003 (2012).

[48] S. Mizukami *et al.*, Phys. Rev. Lett. **106**, 117201 (2011).

[49] J. M. D. Coey, *Magnetism and Magnetic Materials* (Cambridge University Press, 2009).

[50] H. Kurt, K. Rode, P. Stamenov, M. Venkatesan, Y.-C. Lau, E. Fonda, and J. M. D. Coey, Phys. Rev. Lett. **112**, 027201 (2014).

[51] A. K. Nayak *et al.*, "Design of compensated ferrimagnetic Heusler alloys for giant tunable exchange bias," Nat. Mater. (published online, 2015).

[52] P. Entel *et al.*, J. Phys. D: Appl. Phys. **39**, 865 (2006).

[53] P. J. Brown *et al.*, J. Phys.: Condens. Matter **11**, 4715 (1999).

[54] J. Winterlik *et al.*, Adv. Mater. **24**, 6283 (2012).

[55] G. D. Liu *et al.*, Appl. Phys. Lett. **87**, 262504 (2005).

[56] G. D. Liu *et al.*, Phys. Rev. B **74**, 054435 (2006).

[57] J. C. Suits, Solid State Commun. **18**, 423-425 (1976).

[58] S. S. P. Parkin, private communication (2014).

[59] A. K. Nayak, C. S. Mejia, Y. Skourski, C. Felser, and M. Nicklas, Phys. Rev. B **90**, 220408(R) (2014).

[60] A. K. Nayak *et al.*, Phys. Rev. Lett. **110**, 127204 (2013).

[61] O. Meshcheriakova *et al.*, Phys. Rev. Lett. **113**, 087203 (2014).